

Supplementary figures and tables of:

Root-zone carbon and nitrogen pools across two chronosequences of coastal marshes formed using different restoration techniques: Dredge sediment versus river sediment diversion

S. Alex McClellan^{a,*}, Tracy Elsey-Quirk^b, Edward A. Laws^a, Ronald D. DeLaune^b

^a *Department of Environmental Sciences, Louisiana State University, 93 South Quad Dr, Baton Rouge, LA 70803, USA*

^b *Department of Oceanography and Coastal Sciences, Louisiana State University, 93 South Quad Dr, Baton Rouge, LA 70803, USA*

*Corresponding author.

E-mail address: alex.mcclellan@gmail.com (S.A. McClellan).

DOI: <https://doi.org/10.1016/j.ecoleng.2021.106326>

Table S1. Ancillary information for each marsh sampled

Marsh	Coordinates [†]	Average elevation [‡] (NAVD88)	Estimated annual time flooded ^a (%)	Aboveground biomass ^b (g·m ⁻²)
Sabine				
1 year	29°56'48"N, 93°24'39"W	24 ± 3 cm	5–36	994
6 years	29°56'16"N, 93°24'3"W	10 ± 3 cm	22–63	2068
14 years	29°57'42"N, 93°24'47"W	10 ± 3 cm	22–63	1872
33 years	29°55'8"N, 93°20'48"W	32 ± 3 cm	2–23	1196
Reference A	29°55'37"N, 93°26'17"W	13 ± 1 cm	21–55	791
Reference B	29°56'39"N, 93°26'21"W	7 ± 2 cm	30–66	1457
WLD				
16 years	29°30'4"N, 91°28'51"W	2 ± 5 cm	49–87	75
29 years	29°30'45"N, 91°27'56"W	53 ± 2 cm	1–4	335
41 years	29°31'56"N, 91°26'10"W	51 ± 6 cm	1–7	300
Reference	29°33'15"N, 91°25'42"W	50 ± 10 cm	1–4	—

[†] Coordinates of the Sabine marsh plots were selected to match a subset of those sampled by Abbott et al. (2019), which were randomly selected; coordinates of the WLD marsh plots other than the reference were based on Henry and Twilley (2014)—triplicate samples were collected haphazardly within 10 m of these coordinates.

[‡] The elevations of the Sabine marsh plots were determined in 2016 by Abbott (2017) based on in situ real-time kinematic positioning measurements (errors are standard error of triplicate plots). The approximate elevations of the WLD plots are based on digital elevation model data (1-m resolution LiDAR) obtained from the 2012 USGS National Elevation Dataset (USGS, 2012) and averaged over a 10-m² area (± standard deviation). These elevations are relative to the North American Vertical Datum of 1988 (NAVD88).

^a Estimates of the % of time that the marsh surface was fully submerged were made based on the elevations and on historical hourly water level data obtained for years 2010 through 2017 from nearby monitoring stations (Calcasieu Pass and Ameranda Pass; NOAA Open Geospatial Consortium Sensor Observation Service; <https://opendap.co-ops.nos.noaa.gov/ioos-dif-sos/>). For each of the eight years, the number of hours for which the water level equaled or exceeded the marsh elevation was divided by the total number of hourly measurements that year and multiplied by 100%. Each range shown is the minimum and maximum of the eight annual estimates.

^b In Sabine, average estimates of the live aboveground biomass of the sampled marshes were reported by Abbott (2017). In WLD, the live herbaceous aboveground biomass was based on the model dataset of Jensen et al. (2021), averaged over a 10-m² area about the sampling sites. Biomass estimates were not available for the WLD reference site.

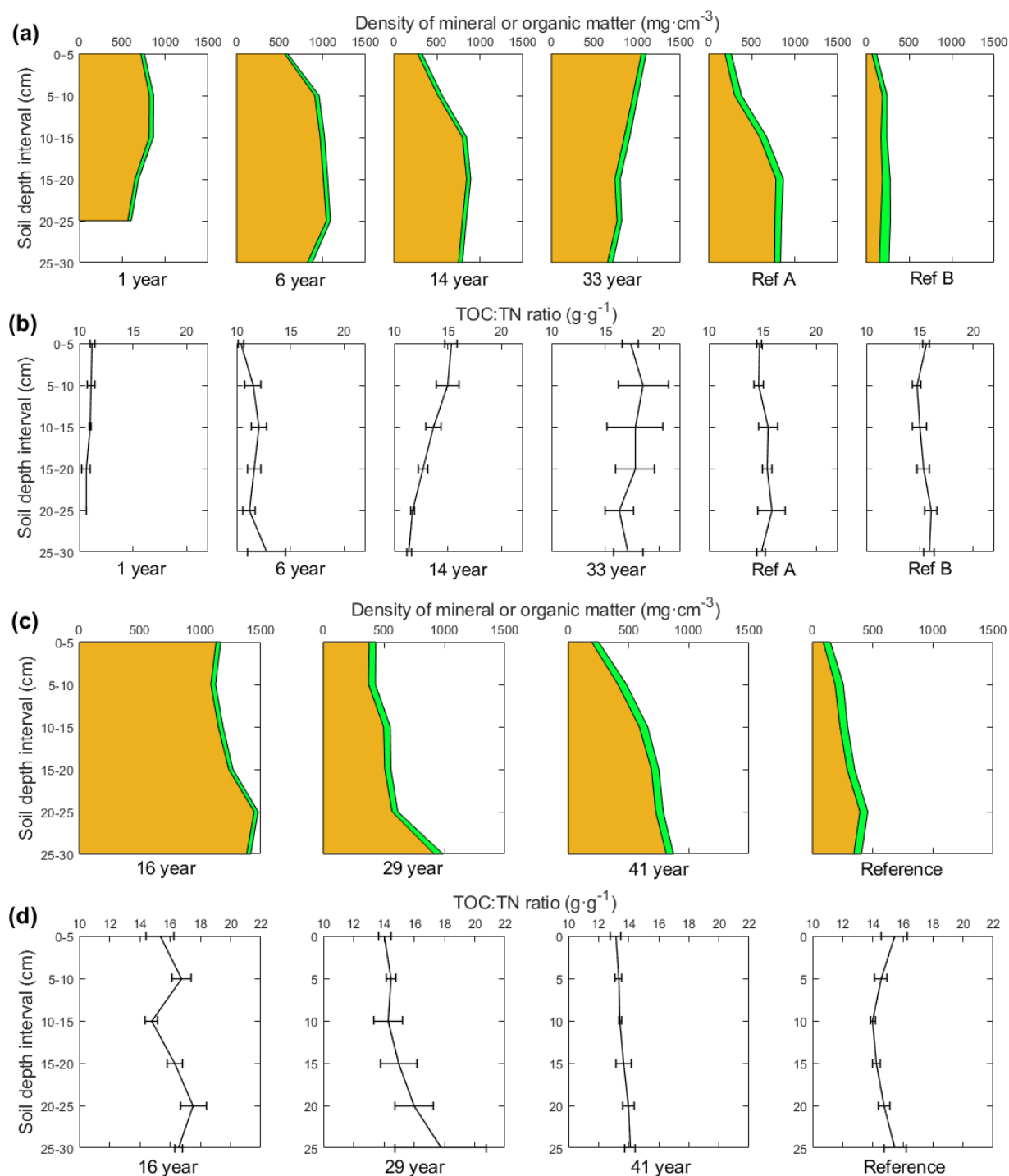


Fig. S1. Average soil core profiles at 5-cm depth intervals: average density of mineral matter (amber) and organic matter (green) in the Sabine (a) and WLD (c) soils; average ratio of TOC:TN in the Sabine (b) and WLD (d) soils. Error bars are \pm standard error ($n = 3$ cores).

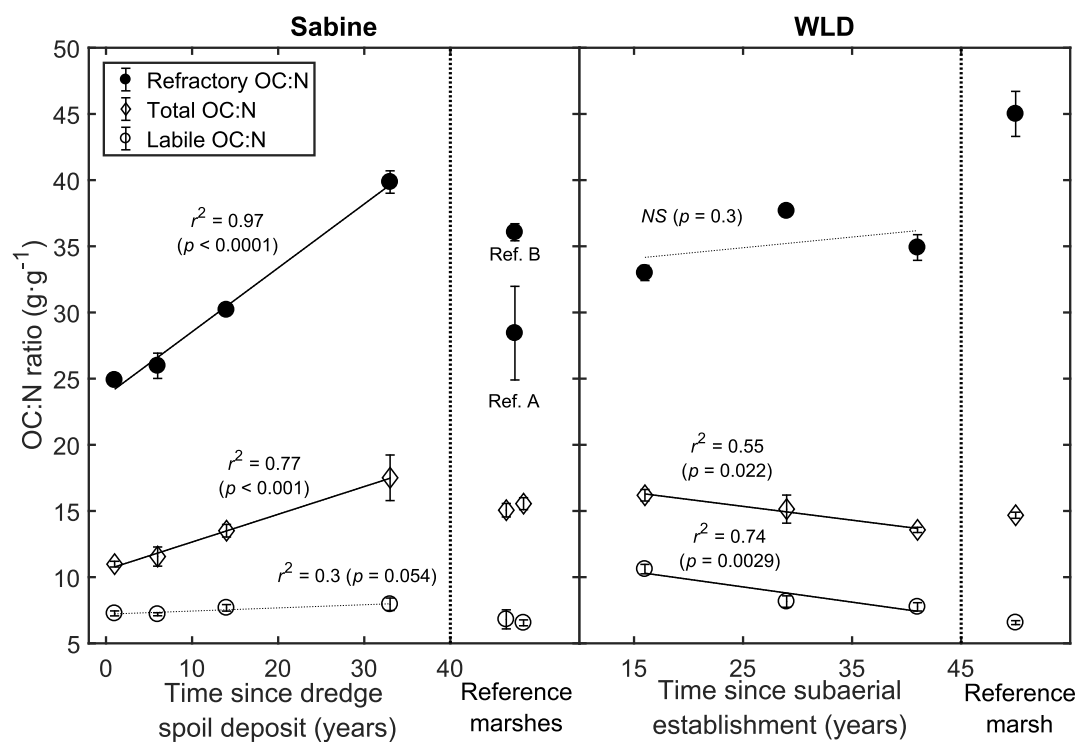


Fig. S2. Organic C to N ratios of the total soil (diamonds), refractory fraction (closed circles), and labile fraction (open circles) as a function of marsh age in Sabine and WLD. Error bars represent \pm standard error ($n = 3$ cores).

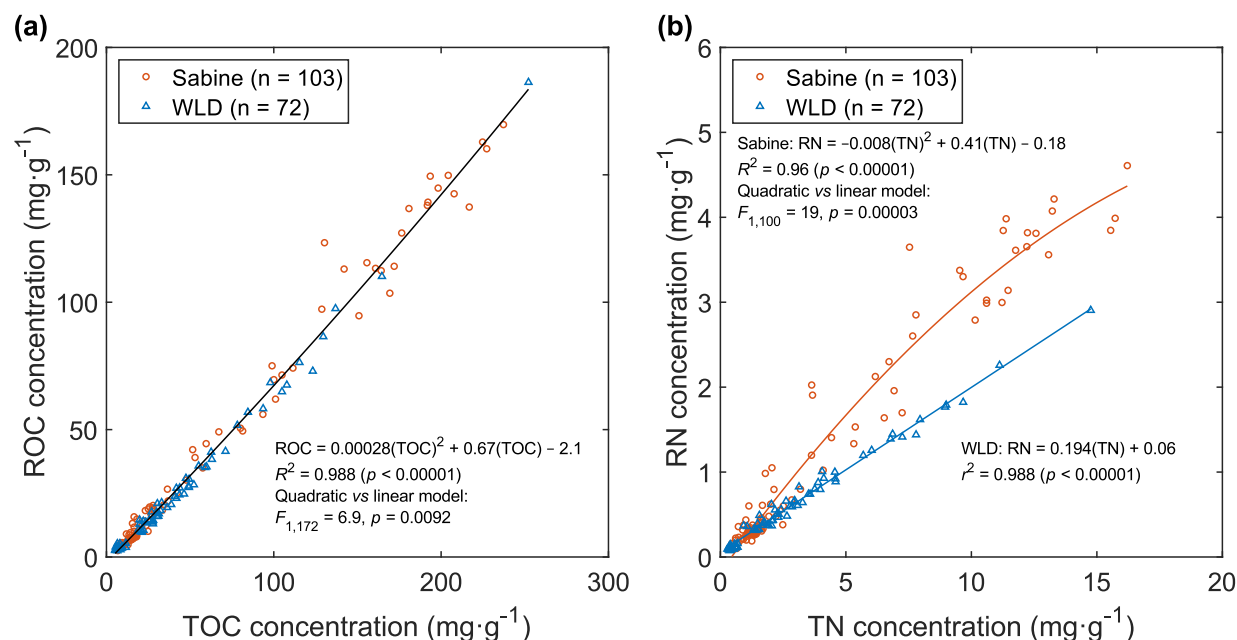


Fig. S3. Correlations between ROC and TOC (a) and between RN and TN (b) among the Sabine and WLD marshes. Data were fit to either a single model or separate models depending on the results of ANCOVA performed on the log-transformed data (Fig. S4).

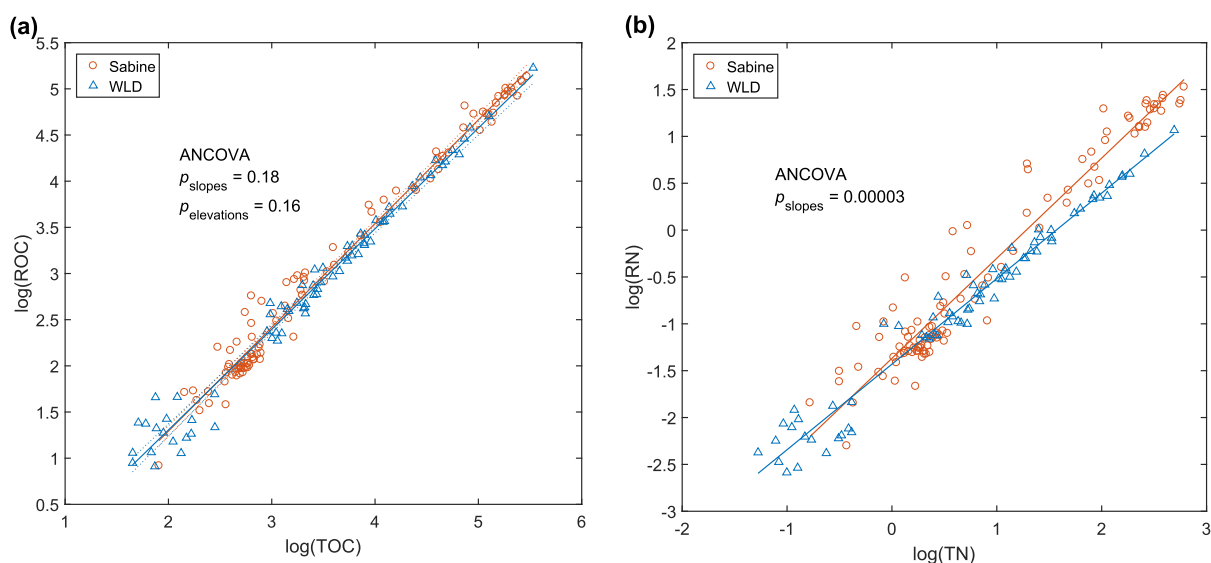


Fig. S4. Log-transformed correlation between TOC and ROC (a) and TN and RN (b), showing separate linear fits and ANCOVA results.

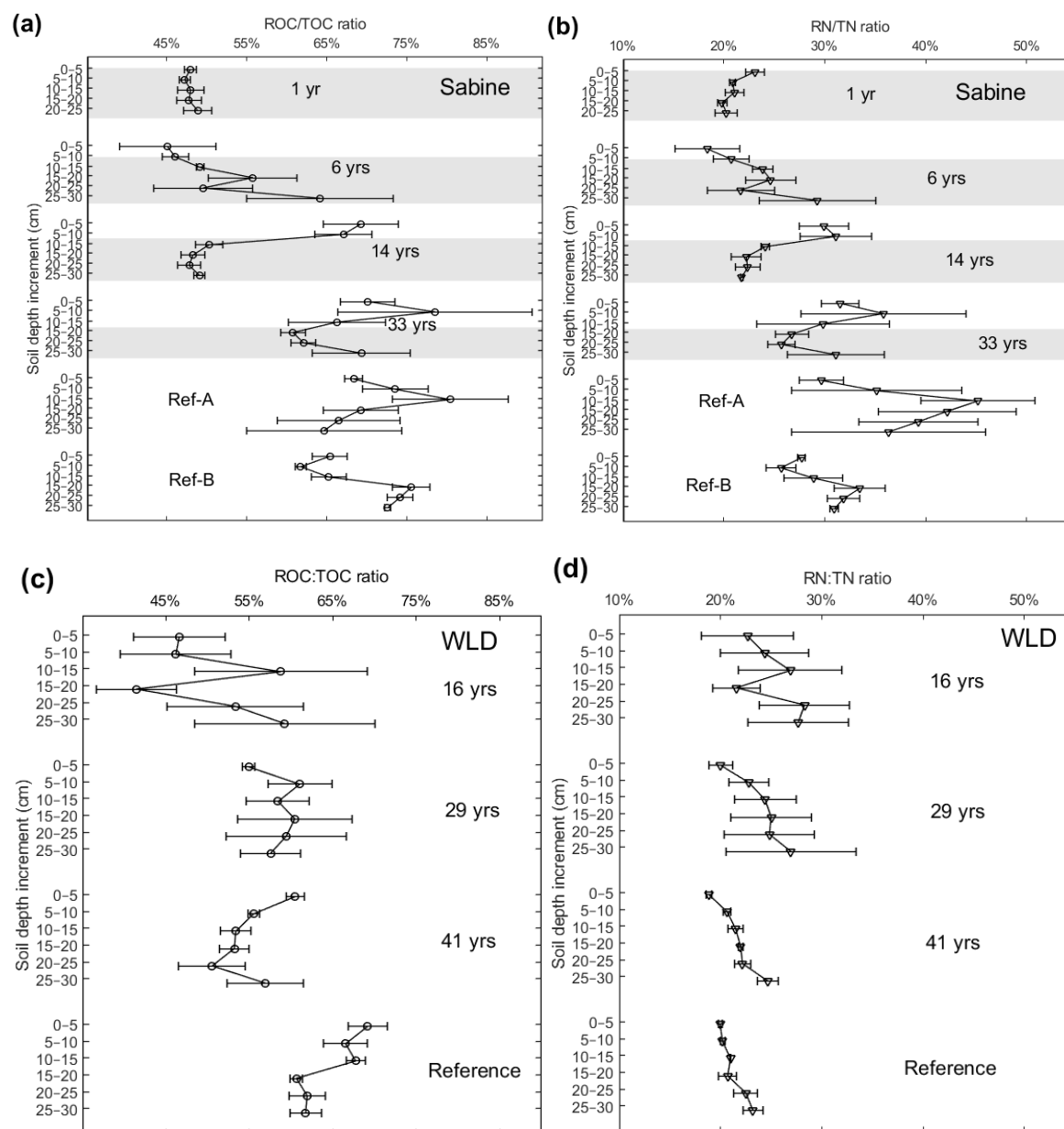


Fig. S5. Depth profiles of the average ROC:TOC ratio (circles) and RN:TN ratios (triangles) in Sabine (a and b) and WLD (c and d). Error bars are \pm standard error (n = 3 cores). Shading in (a) and (b) represents the estimated depth intervals that were composed of dredge spoil material based on previous observations (Abbott et al., 2019).

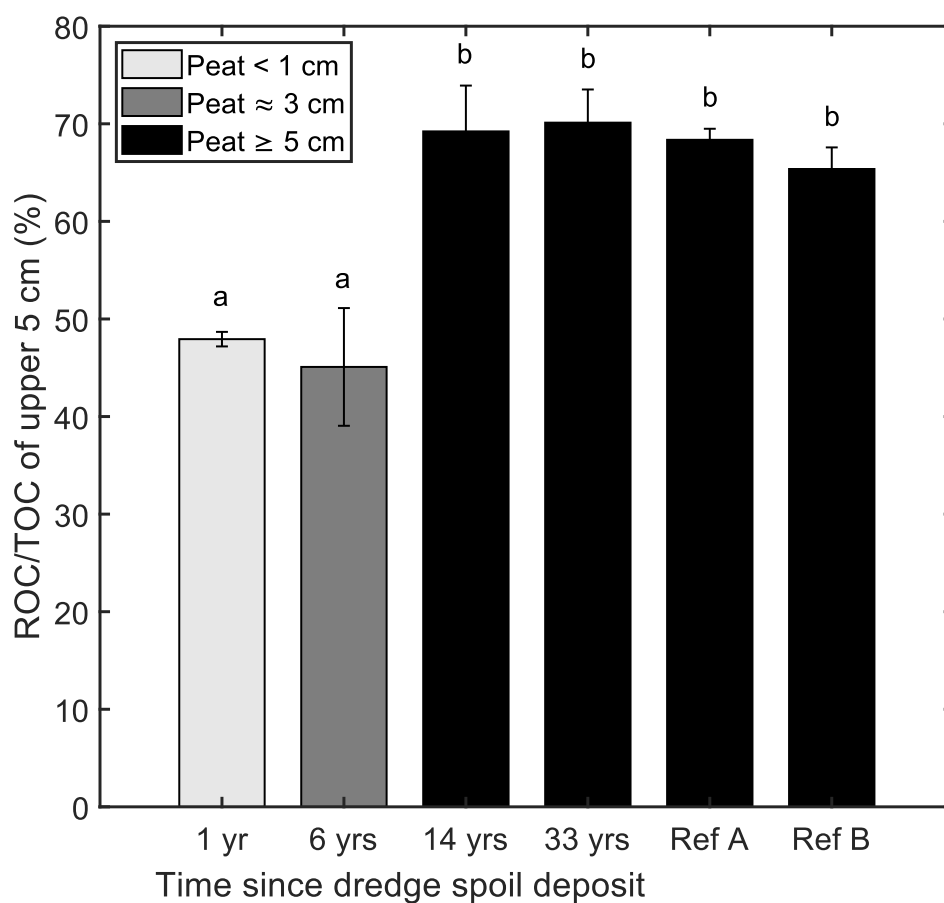


Fig. S6. Comparison of the average ROC/TOC ratios of the top 5 cm of soil in each of the Sabine marshes. The shading of the bars corresponds to the estimated depth of the peat layer. In the created marshes, the sediment below this layer is expected to be composed almost entirely of dredge spoil material. The letters indicate significant differences ($\alpha = 0.05$) based on Tukey-Kramer honestly significant difference post-hoc tests following a one-way ANOVA.

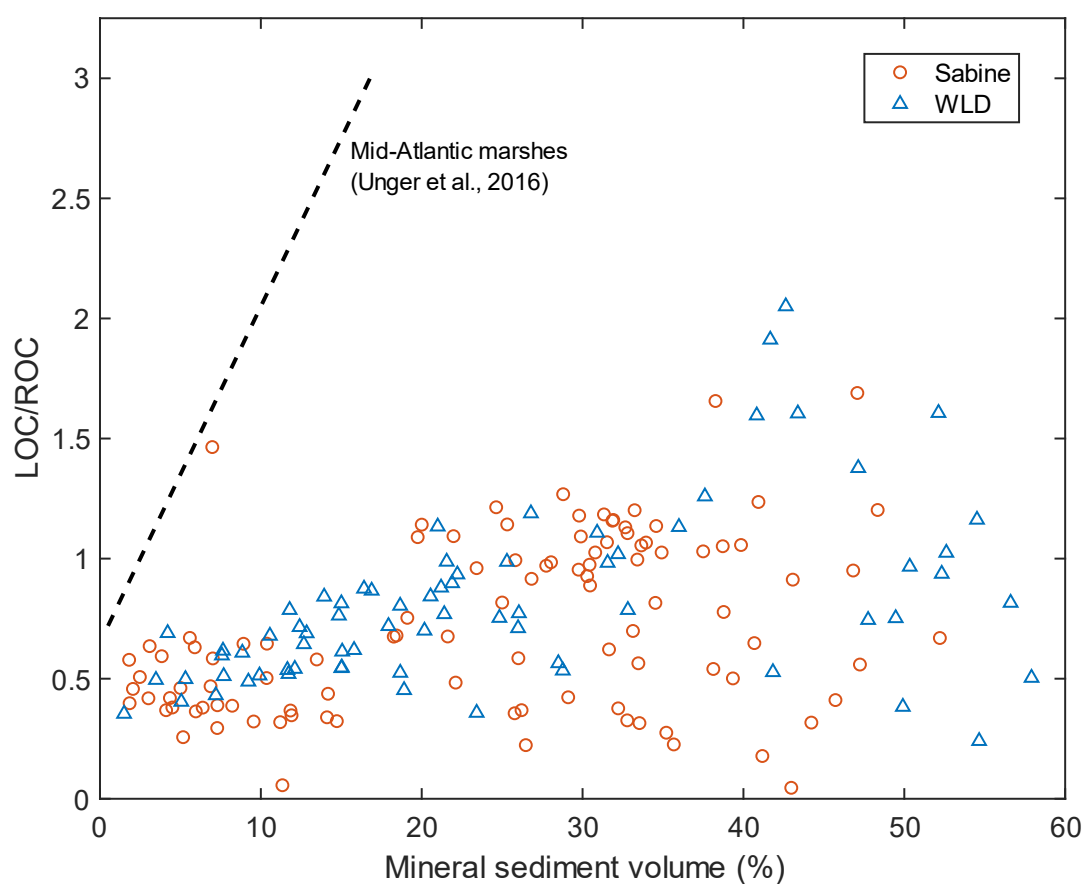


Fig. S7. Plot of the LOC:ROC ratios versus mineral sediment volume for the individual soil core sections of Sabine and WLD (markers). The dashed line is based on the linear regression equation reported for marshes on the mid-Atlantic US coast (Unger et al., 2016). For the purposes of comparison, the percent of soil volume accounted for by mineral sediment of the Sabine and WLD samples was approximated by dividing the respective mineral sediment densities by the assumed particle density of the mineral fraction ($2.61 \text{ g}\cdot\text{cm}^{-3}$; DeLaune et al., 1983) and multiplying by 100.

References

- Abbott, K.M., 2017. Blue carbon accumulation and microbial community composition in a chronosequence of created coastal marshes in the Chenier Plain, Louisiana. Louisiana State University: Master's Theses. 4509.
- Abbott, K.M., Elsey-Quirk, T., DeLaune, R.D., 2019. Factors influencing blue carbon accumulation across a 32-year chronosequence of created coastal marshes. *Ecosphere*. 10:e02828. <https://doi.org/10.1002/ecs2.2828>.
- DeLaune, R.D., Baumann, R.H., Gosselink, J.G., 1983. Relationships among vertical accretion, coastal submergence, and erosion in a Louisiana Gulf Coast marsh. *Journal of Sedimentary Research*. 53:147-157. <https://doi.org/10.1306/212f8175-2b24-11d7-8648000102c1865d>.
- Henry, K.M., Twilley, R.R., 2014. Nutrient biogeochemistry during the early stages of delta development in the Mississippi River Deltaic Plain. *Ecosystems*. 17:327-343. <https://doi.org/10.1007/s10021-013-9727-3>.
- Jensen, D.J., Simard, M., Twilley, R., Castaneda, E., McCall, A., 2021. Pre-Delta-X: Aboveground biomass and vegetation maps, Wax Lake Delta, LA, USA, 2016. <https://doi.org/10.3334/ORNLDAAAC/1821>.
- Unger, V., Elsey-Quirk, T., Sommerfield, C., Velinsky, D., 2016. Stability of organic carbon accumulating in *Spartina alterniflora*-dominated salt marshes of the mid-Atlantic U.S. *Estuarine, Coastal and Shelf Science*. 182:179-189. <https://doi.org/10.1016/j.ecss.2016.10.001>.
- USGS, 2012. U.S. Geological Survey 20200330: One-meter x65y327 and One-meter x64y327 LA Atchafalaya2. ScienceBase-Catalog Version: 2.177.1. <https://www.sciencebase.gov/catalog/item/5ead02a782cefae35a252ccb> <https://www.sciencebase.gov/catalog/item/5ead01d082cefae35a252861>